An Investigation of CaO Sulfation Mechanisms in Boiler Sorbent Injection

A laboratory differential reactor study was conducted at temperatures of 975-1,275 K to investigate CaO sulfation mechanisms with calcine (CaO) samples derived from pulverized limestones and dolomites, and hydrated limes. The limestones had 8-115 μm mean particle sizes, a range applicable for boiler sorbent injection for SO_2 control. Under conditions applicable for boiler sorbent injection, the sorbent performance, in terms of initial reaction rate and saturation utilization, was limited by the SO_2 pore diffusion rate and by premature pore mouth plugging by $CaSO_4$ product and, thus, depended on CaO particle size and pore size. Hydrated lime and Na_2CO_3-promoted limestones showed performance superior to that of limestones, because they produced calcines with larger pores. Intrinsic reaction rate as reported by Borgwardt and Bruce (1986) was observed at temperatures below 1,100 K.

Mark R. Stouffer
Heeyoung Yoon
Consolidation Coal Company
Research & Development
Library, PA 15129

Introduction

Boiler sorbent injection is a low capital cost option for retrofit flue gas SO_2 control. It involves injection of a calcium-based sorbent (e.g., pulverized limestone or hydrated lime) into the high-temperature (approximately 1,250–1,600 K) regions of a coal-fired boiler. At these temperatures, the sorbent is rapidly calcined to form CaO, which subsequently undergoes sulfation to $CaSO_4$. Although reaction of SO_2 with the limestone is possible, the rapidity of calcination makes the sequential reaction most likely. Pilot and industrial tests of boiler limestone injection have demonstrated SO_2 reductions of 50% or higher at sorbent utilization efficiencies ranging from 15 to 20% (Fink et al., 1984). This low sorbent utilization offers the opportunity for significant process improvement.

The sulfation reaction involves complex chemical and physician phenomena, such as the intrinsic chemical reaction, various gas and solid diffusional processes, and pore plugging by reaction product. The sulfation reaction has been widely studied, especially under conditions applicable to the fluidized bed combustion process (e.g., Potter, 1969; Borgwardt, 1979; Borgwardt and Harvey, 1972; Pigford and Sliger, 1973; Hartman and Coughlin, 1974, 1976; James and Hughes, 1976; Dogu, 1981; Bardakci, 1984; Chang and Thodos, 1984; Ciambelli et al., 1985). Published experimental data from many of these studies are limited to relatively large calcine particles (~1 mm) with low surface areas (<5 m^2/g) and low reaction temperatures (<1,120 K), and to nondispersed reaction systems. Reaction rates measured under the above conditions are too low to account for the significant sorbent reactivity observed in the very short contact time (a few seconds or less) in boiler tests. More recent experimental studies (Borgwardt, 1985; Borgwardt et al., 1986) conducted with very fine (~1 μm) limestone particles showed that extremely high CaO surface areas (up to 90 m^2/g) are produced when fine limestone is calcined in a well-dispersed reaction system. Additional studies (Borgwardt and Bruce, 1986; Borgwardt et al., 1987) showed that sulfation activity of 1 μm CaO particles increases with the square of their BET surface area. These results may account for the high sorbent reactivity observed in boiler tests.

A calcine particle produced from $CaCO_3$ or $Ca(OH)_2$ in a dispersed system may be regarded as an aggregate of many nonporous grains of CaO, surrounded by intraparticle void spaces (or pores), Figure 1. To account for reported high-calcine surface areas, these grains must be quite small (e.g., as small as ~20 nm in diameter). The reaction of such a calcine particle with SO_2 involves the following rate processes: diffusion of SO_2/O_2 through the bulk gas to the particle surface, diffusion of SO_2/O_2 through the pores (intergranular voids) to the grain surfaces, adsorption of the gaseous species on the grain surfaces, diffusion of reacting species through the $CaSO_4$ product layer at the grain surfaces, and chemical reaction. Borgwardt and Bruce (1986) showed that, in the absence of bulk and pore diffusion resistances, sulfation is controlled by product-layer diffusion at the grain surfaces. The following model was reported for the intrinsic CaO reaction rate, that is, the rate in the absence of gas

---

Correspondence concerning this paper should be addressed to M. R. Stouffer.

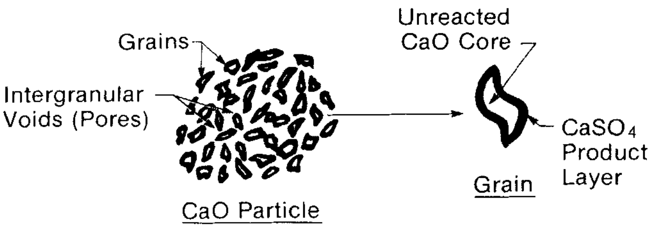

Figure 1. CaO particle.

phase diffusional resistances.

$$1 - 3(1 - X)^{2/3} + 2(1 - X) = k_d \cdot t \tag{1}$$

$$k_d = 2.65(S)^2(P_{SO_2})^n \exp(-E/RT) \tag{2}$$

This model is based on the unreacted core model (Levenspiel, 1972; Szekely, 1976) with product-layer diffusion as the limiting resistance. The model equation indicates that the reaction rate is proportional to the square of the CaO BET surface area (S). The activation energy (E) was determined to be 153 kJ/mol (36.6 kcal/mol) and the reaction order in SO_2 partial pressure (n) was determined to be 0.62. Based on the reaction order and the high temperature sensitivity, it was concluded that the product-layer diffusion occurs through a solid-state ionic diffusion process.

The product-layer diffusivity (D_s) has been calculated based on observed rate data (Borgwardt et al., 1987) for CaO derived from six different limestones and six different hydrated limes. At 1,073 K, 304-Pa SO_2, and with about the same 22 m^2/g average BET surface area, the diffusivities ranged from 1.2×10^{-12} to 3.2×12^{-12} m^2/s for the CaO samples derived from natural limestones and from 1.4×10^{-12} to 2.7×10^{-12} m^2/s for the hydrate-derived samples. In the calculation of the product-layer diffusivities, Borgwardt et al. used the random pore model of Bhatia and Perlmutter (1981), rather than the unreacted core model above. The above results indicated that the activity of CaO in the absence of pore diffusion resistance is about the same whether derived from limestone or hydrated lime. These results do not explain many recent observations in pilot-scale tests that hydrated sorbents are more reactive than limestones for boiler sorbent injection (e.g., Beittel et al., 1985; Bortz and Flament, 1985; Cole et al., 1986; Kirschgessner and Gullett, 1986; Snow et al., 1986).

Prior to the sulfation mechanism study reported here, an extensive laboratory calcination study was conducted using the same test sorbents (Stouffer and Yoon, 1986). This work determined calcination kinetics as well as the effects of calcination conditions on calcine physical properties. For the commerical limestone samples having a size range applicable to boiler injection, calcination in a well-dispersed system (i.e., the differential reactor) produced calcines with BET surface areas ranging up to 70 m^2/g. The observed surface areas were in the same range reported by Borgwardt (1985) and Borgwardt et al. (1986) for 1-μm limestone particles. These results indicate that calcine intermediates in the boiler injection process may have high surface areas. Calcine surface area depended on calcination temperature and contact time, CO_2 partial pressure, and the source limestone. This information was used for generating CaO samples for the present sulfation study.

In the current study, the mechanisms and rate-controlling steps for the CaO/SO_2 reaction were investigated for CaO particle sizes applicable to boiler sorbent injection. This study provides information on the effects of pore diffusion and pore mouth plugging on sulfation. The test variables were calcine physical properties (particle size, surface area, and pore structure), reaction temperature, SO_2 concentration, and the concentration of different alkali additives applied to the limestone prior to calcination. Calcine physical properties were varied by using different calcination conditions and different CaO precursors. The test temperature range was from 975 to 1,275 K, at the low end of the range appropriate for boiler injection (about 1,150 to 1,500 K). Calcines from 11 commercially available sorbents were tested. The sorbents included seven pulverized limestones, two pulverized dolomitic stones, and two hydrated sorbents. A laboratory differential reactor was used to measure the sulfation rate and saturation calcium utilization.

Experimental Studies

Test Sorbents

Table 1 shows chemical and physical analyses of 12 sorbents used for this study. They include seven limestones, one pure $CaCO_3$, two dolomitic stones, a hydrated lime, and a pressure-hydrated dolomitic lime. All were commercially available and potential candidate sorbents for boiler injection, except for Sorbent No. 8, a high-purity, reagent-grade, precipitated $CaCO_3$.

The limestones and dolomitic stones had a significant variation in particle-size distribution with the mean diameters ranging from 8.4 to 115 μm (specific surface mean). The BET specific surface areas ranged from 0.3 to 6.3 m^2/g for these stones. BET surface areas were 21 and 23 m^2/g for the hydrated sorbents.

Much of the sulfation kinetic data were generated with calcines from one stone, the Dravo Maysville – 100 mesh limestone (Sorbent No. 1). Other sorbents were tested for comparison.

Differential reactor

A fixed-bed differential reactor (Figure 2) used for the tests was similar to that described by Borgwardt et al. (1986). The test unit allowed control of isothermal reaction temperature to within ±3 K up to 1,300 K and control of the CaO contact time with SO_2 to about ±1 s. To maintain differential sulfation conditions with respect to SO_2 partial pressure and temperature and to eliminate bulk gas mass transfer resistance, very small sorbent charges (down to 8 mg) were well-dispersed in quartz wool and were swept with large flows (up to 2 m^3/h standard) of simulated flue gas. Differential conditions were not possible above about 1,225 K because of high sulfation rates. A few tests at 1,275 K provided saturated sorbent utilization data, but no accurate rate data.

Test Procedures

Calcine preparation

Before sulfation rate measurement, the sorbent sample was calcined under controlled conditions.

For each of the test sorbents, tests were conducted in which the sorbent was calcined in the differential reactor immediately prior to sulfation. This produced very high surface area calcines (35 to 70 m^2/g). The sorbent particles were dispersed in a quartz wool matrix and contacted by a flow of air. The calcination tem-

Table 1. Test Sorbents

No.	Sorbent	Elemental Analysis of 1,200 K Ash CaO wt. %	 MgO wt. %	Average Particle Dia. μm* Mass Median	 Specific Surface Mean**	BET† Surface Area of Raw Sorbent, m^2/g
1	Dravo Maysville Limestone, -100 mesh	50.8	2.74	28.3	13.4	1.4
2	Dravo Maysville Limestone, -325 mesh	51.9	2.81	7.2	8.5	6.3
3	Pfizer Marble White 200 Limestone	54.8	0.4	23.1	14.6	0.7
4	Warner Bell Mine Limestone	54.7	0.6	25.9	15.8	1.8
5	Mississippi R-1 Limestone	55.2	0.3	300.0	112.0	0.9
6	Genstar Apex Limestone	56.5	0.5	28.3	16.1	1.0
7	Utah Marblehead Limestone	56.6	0.3	48.0	27.0	0.9
8	Baker Reagent $CaCO_3$	56.5	0.0	13.2	11.2	0.5
9	Hommel #1974 Dolomite	32.0	20.1	32.9	22.0	0.8
10	Warner Dolomite	28.9	22.0	98.2	55.8	0.3
11	Dravo Longview Hydrated Lime	72.0	2.4	‡	‡	21.1
12	Pressure Hydrated Dolomite	41.7	30.4	‡	‡	23.3

*Particle size determined by wet screening and by Coulter Counter.
**Specific surface mean, $D_p = (\Sigma Yi)/(\Sigma Yi/Di)$, and where Yi = weight fraction of size cut and Di = Average diameter of size cut.
†Surface areas determined by N_2 adsorption and one-point BET method.
‡Reliable particle size data not available for hydrated sorbents.

perature was controlled at the same temperature as for the subsequent sulfation. The contact time was set at about that required for complete calcination in order to develop the maximum calcine surface area. Based on previous calcination data (Stouffer and Yoon, 1986), the calcine surface area reaches a maximum at about the point of complete calcination, followed by a gradual drop in surface area with further contact (Figure 3). Because of the temperature dependence of the calcination rate, shorter contact times were required for complete calcination at higher temperature. For a given sorbent sample, the maximum calcine surface area was nearly independent of calcination temperature (Figure 3). The maximum calcine surface area depended on the source sorbent (Table 2), varying from 35 to 70 m^2/g among the ten calcitic and dolomitic limestones tested, and 40 to 45 m^2/g for the two hydrated sorbents tested.

For one sorbent, the Dravo Maysville Limestone (No. 1), tests were conducted for calcines with a range of surface areas. For tests with low surface area calcines (less than 20 m^2/g), limestone samples were calcined externally in a muffle furnace in 1- to 2-g batches. Calcination under these nondifferential, nondispersed conditions yielded low surface area calcines. For tests with intermediate surface area calcines (20 to 35 m^2/g), samples were calcined in the differential reactor, and the contact time was extended after complete calcination (to 30 minutes to one hour or more).

Surface area and pore volume distributions of the CaO intermediates were determined by producing calcine samples under conditions duplicating those used prior to sulfation. Calcine surface areas were measured by N_2 adsorption at 77 K and the one-

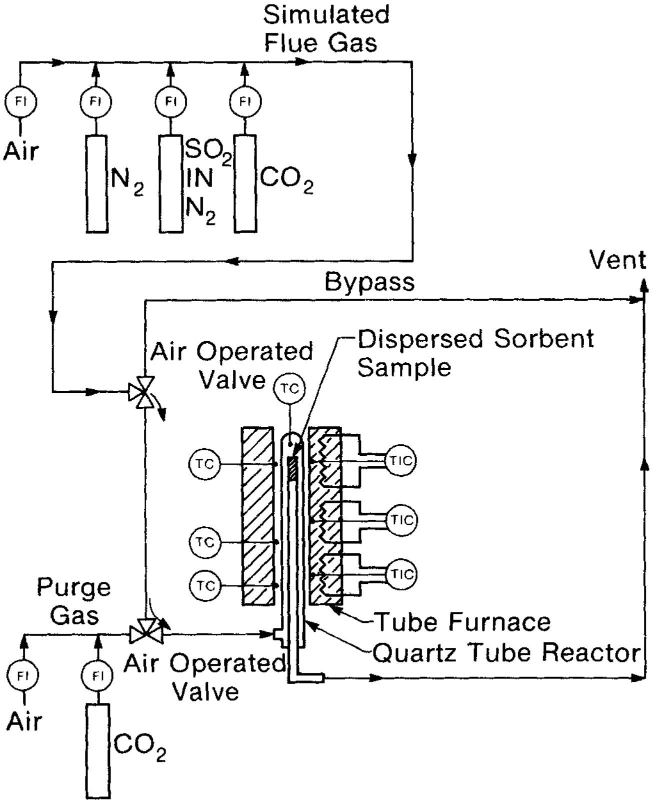

Figure 2. Differential reactor test unit.

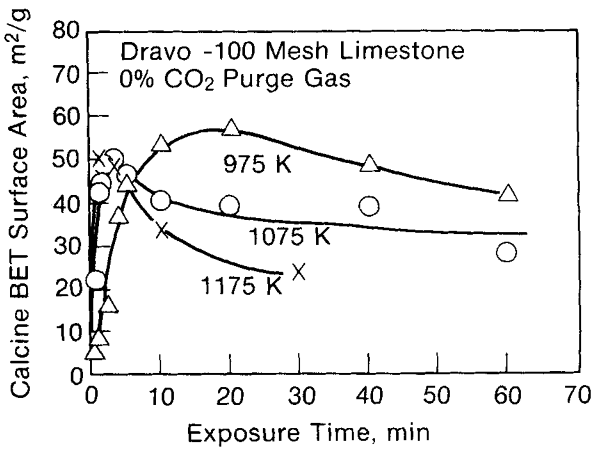

Figure 3. Dependence of calcine BET surface area on calcination temperature/contact time.

Table 2. Maximum Calcine Surface Areas

No.	Sorbent	Max. BET Surface Area of Calcine m^2/g
1	Dravo Maysville Limestone, -100 mesh	50–55
2	Dravo Maysville Limestone, -325 mesh	35
3	Pfizer Marble White 200 Limestone	60
4	Warner Bell Mine Limestone	45
5	Mississippi R-1 Limestone	70
6	Genstar Apex Limestone	60
7	Utah Marblehead Limestone	65
8	Baker Reagent $CaCo_3$	55
9	Hommel #1974 Dolomite	70
10	Warner Dolomite	70
11	Dravo Longview Hydrated Lime	40
12	Pressure Hydrated Dolomite	45

point BET method. Pore distributions were determined from N_2 desorption isotherms (77 K), following the methods of Barrett et al. (1951).

Preparation of additive promoted sorbents

Tests were conducted with an additive (Na_2CO_3, NaCl, $CaCl_2$, or $FeCl_3$) added to limestone prior to calcination. For most of these tests, the promoted limestone sample was prepared by adding an aqueous additive solution to a limestone/water slurry with vigorous mixing, followed by evaporation of water from the combined slurry to form a dry product. For a few of the tests, the additive was finely ground and mixed in dry form with the pulverized limestone. After preparation of the promoted limestone, the sample was calcined in the differential reactor as described previously. The calcination time was set for complete calcination.

Sulfation rate measurement

After calcination, the differential reactor was used to contact the CaO sample with a simulated flue gas stream, typically containing 80% N_2, 15% CO_2, 5%, O_2, and 750–3,000 ppm SO_2. Immediately after a set reaction time between 5 and 600 s, the SO_2-containing gas was shut off, and the quartz holder was removed quickly from the furnace and cooled by a water spray on the exterior tube surface. The entire quartz wool bed was removed from the quartz holder and analyzed. The conversion of CaO to $CaSO_4$ was determined by the Ca and S contents in the recovered sample, measured by atomic adsorption spectroscopy and combustion infrared detection (Leco Analyzer), respectively. A series of such runs were conducted for each sorbent in order to develop a conversion vs. time response at constant flue gas conditions. Data from short contact time runs were used to determine the initial sulfation rate, that is, the reaction rate over the first 15% conversion. Data from runs at long contact times were used to determine saturation calcium utilization.

Data reproducibility

Table 3 shows reproducibility of the calcium conversion data in sets of repeat runs with and without additive promotion. The average deviations from the mean were less than 2% (absolute) in all runs but one. The results indicate that the calcination procedure, the sulfation procedure, the solids analyses, and the additive treatment procedure were reproducible.

Table 3. Reproducibility of Calcium Conversion Data

Sulfation Contact Time, s	Run 1 %	Run 2 %	Run 3 %	Avg. Dev. from Mean, %
Case I Limestone: Dravo Maysville Limestone, -100 mesh Calcination/Sulfation Temperature: 1,075 K Calcine Surface Area: 50 m^2/g Additive: None				
10	10.5	11.5		0.5
20	13.0	15.0		1.0
30	20.0	19.0		0.5
60	24.0	23.5		0.3
300	33.0	37.0		2.0
Case II Limestone: Dravo Maysville Limestone, -100 mesh Calcination/Sulfation Temperature: 1,175 K Additive: 2 wt. % Na_2CO_3				
5	—	6.5	7.0, 7.5	0.3
10	21	20	19	0.7
20	24	—	33	4.3
30	28	30	31	1.1
60	—	40	44	1.8
300	50	52	53	1.2

Results and Discussion

Intrinsic sulfation rate

Intrinsic sulfation rate data (that is, reaction rates in the absence of gas-phase diffusional resistances) confirm the rate model of Borgwardt and Bruce (1986), and support their conclusion that, at the grain surfaces, sulfation is controlled by product-layer diffusion. Figure 4 shows a comparison of the measured sulfation data for calcines from Dravo −100 mesh limestone with Borgwardt's unreacted core model predictions

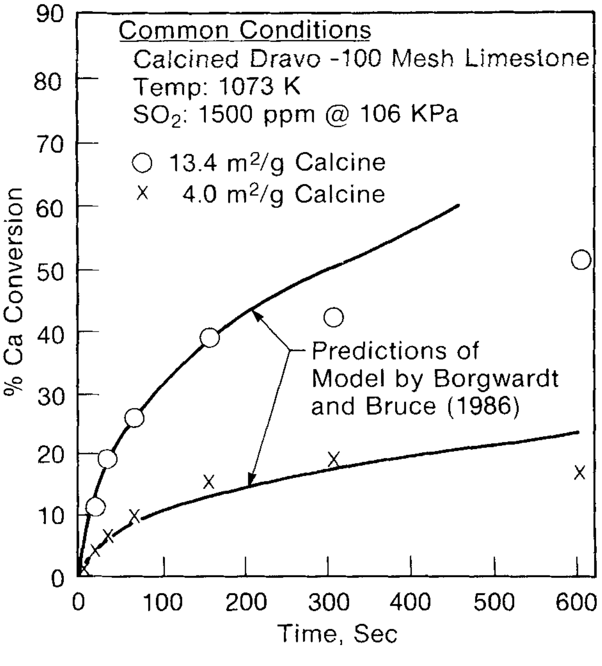

Figure 4. Correlation between sulfation rate model and sulfation rate data measured in the absence of pore diffusion limitation.

(Eq. 1 and 2). At 1,075 K and with 4.0 and 13.4 m^2/g calcines, the model fit the test data well up to about 40% calcium conversion. At higher conversions, the model overpredicted the test data, possibly indicative of plugging of intergranular voids or grain expansion associated with $CaSO_4$ formation.

Diffusion coefficients for the product layer were calculated using the sulfation data for Dravo Maysville limestone. In the unreacted core model with product layer diffusion as the limiting resistance, the product layer diffusivity (D_s) is defined by:

$$k_d = \frac{2\rho MCS^2 D_s}{3} \tag{3}$$

and follows an Arrhenius temperature dependence

$$D_s = D_o e^{-E/RT} \tag{4}$$

At 1,075 K, diffusivities calculated using Eqs. 1 and 3 for the data in Figure 4 (between 5% and 45% calcium conversion) were 6.5×10^{-13} m^2/s for the 4.0 m^2/g calcine and 7.3×10^{-13} m^2/s for the 13.4 m^2/g calcine. These values are lower than the range of 1.2×10^{-12} m^2/s to 3.2×10^{-12} m^2/s reported by Borgwardt et al. (1987) at 1,075 K. However, for the diffusivity calculation, Borgwardt used a model formulated by Bhatia and Perlmutter (1981) instead of the unreacted core model. Using the same calculation method as Borgwardt et al. (1987), the average diffusivity (D_s) calculated for the data in Figure 4 was 2.2×10^{-12} m^2/s, which is within the range reported by Borgwardt.

In the development of the rate model reported above (Eqs. 1 and 2), Borgwardt used 1-μm CaO particles to effectively eliminate pore diffusion resistances. In the current work with larger particles, the intrinsic rate data were measured at reaction temperatures of 1,075 K or lower, and for calcine surface areas lower than 15 m^2/g. At higher temperatures and with higher surface area calcines, measured initial sulfation rates deviated substantially from the above rate model due to pore diffusion effects, as detailed below.

Pore diffusion resistance

At higher temperatures more applicable to boiler sorbent injection (greater than 1,075 K), the initial reaction rates of calcines with greater than 15 m^2/g surface area were significantly lower than predicted by the intrinsic rate model, because the observed rates were limited by pore diffusion. For some calcines, the observed rates were further lowered because of pore mouth plugging by the $CaSO_4$ product. As discussed above, the gaseous reactants, SO_2 and O_2, must diffuse through the bulk gas film and intergranular void spaces (or pores) before reacting with CaO grains. As discussed below, the strong pore diffusion limitation was evidenced by the observed initial reaction rate dependence on temperature, SO_2 partial pressure, particle size, and calcine surface area and pore structure. In the differential reactor, bulk gas diffusion resistance was eliminated by operating with a suitably high reaction gas velocity.

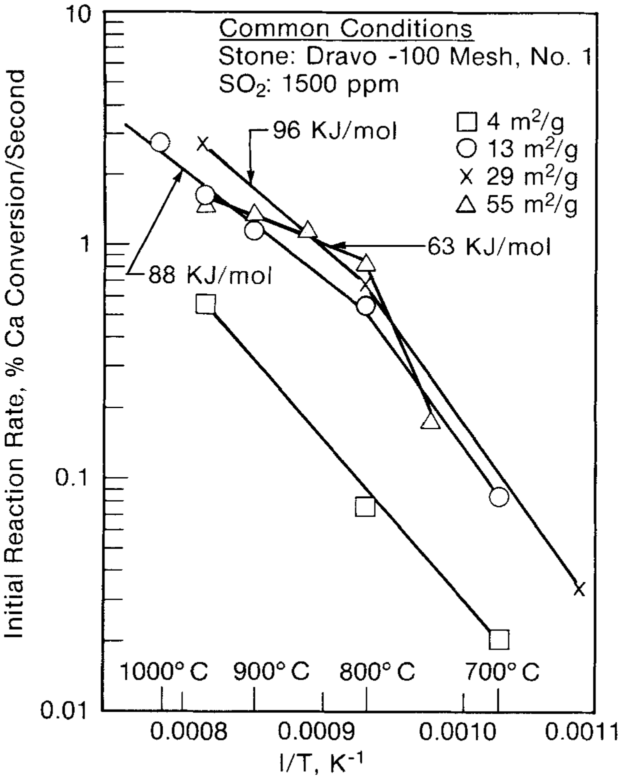

Figure 5. Sulfation temperature dependence.

Figure 5 shows that for higher surface area calcines derived from the Dravo −100 mesh limestone, the apparent activation energy (E_a) dropped to a 63-96 kJ/mol range at higher temperatures. This reduction in the apparent activation energy to roughly one half of the intrinsic activation energy (that measured in the absence of pore diffusion resistance) of 153 kJ/mol was consistent with the theoretical derivation under strong pore diffusion limitation

$$E_a = \frac{E + E_d}{2} \approx \frac{E}{2}$$

assuming $E_d \ll E$. The onset of pore diffusion control for higher surface area calcines (>15 m^2/g) was around 1,075 K, based on the shifts in the slope of the Arrhenius plots shown in Figure 5. For a low surface area calcine (4 m^2/g), transition to pore diffusion control was not evident up to 1,225 K.

The reaction order (n) in SO_2 partial pressure at 1,175 K with 50–55 m^2/g calcines (from Dravo −100 mesh limestone) was estimated at 0.9. Observed initial reaction rates were 0.006, 0.009, and 0.02 s^{-1} at 750, 1,500 and 3,000 ppm SO_2 concentrations, respectively. This value of n contrasts with the value of $n = 0.62$ in the intrinsic kinetic model equation. This change in the reaction order was also indicative of the pore diffusion control, since an nth-order reaction behaves like a reaction of order $(n + 1)/2$ under pore diffusion control (Levenspiel, 1972).

Figure 6 shows that the initial sulfation rates varied roughly inversely with mean particle size. This is another indication that pore diffusion was the rate-controlling step under the test conditions (Levenspiel, 1972). The different sorbent samples (Nos. 1 through 10, Table 1) provided the particle-size variation in the figure.

Calcine pore mouth plugging

Calcine pore mouth plugging by product $CaSO_4$ limited sulfation of highly porous calcines at higher temperatures. The limi-

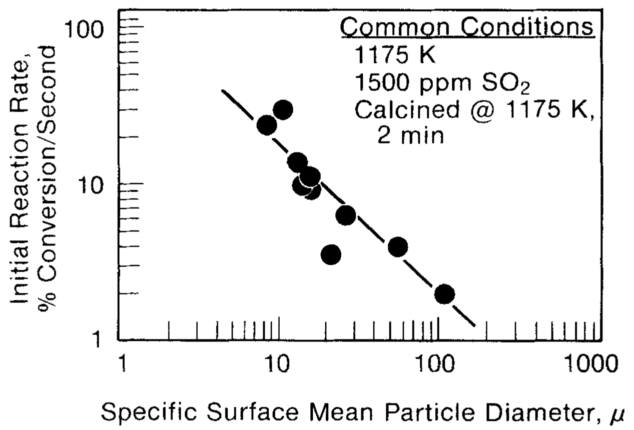

Figure 6. Effect of particle size on sulfation rate with pore diffusion limitation.

tations by pore mouth plugging was evident in the laboratory tests from the exceptionally low apparent activation energies (e.g., <20 kJ/mol) observed with some very high surface area calcines and from reduction in the saturated calcium utilizations with increasing sulfation temperature observed for most of the calcines.

Porous calcines are subject to plugging by product sulfate because the molar volume of $CaSO_4$ (52.2 cm^3/mol; as reported by Hartman, 1976) is considerably greater than that of CaO (16.9 cm^3/mol; as reported by Hartman, 1976). Figure 7 shows the calculated maximum utilization of a constant-sized CaO particle as a function of its porosity, if the utilization is limited by the available pore space for $CaSO_4$ product. However, the sorbent utilization may not reach this calculated maximum, if the mouths of the calcine pores are plugged before the interior of the pores are filled. Pore plugging can reduce the initial sulfation rate as well by increasing the pore diffusional resistance and by reducing the available CaO surface area. Severe pore mouth plugging is most likely when the intrinsic rate of sulfation far exceeds the rate of diffusion of reactants through the pores. Therefore, the degree of deactivation by pore plugging can be expected to increase with increasing temperature because the intrinsic sulfation rate increases more rapidly with temperature ($E = 153$ kJ/mol) than does the gas diffusion rate (E_d typically less than 20 kJ/mol). Because of this temperature effect, premature pore plugging can reduce the apparent activation energy for sulfation. Deactivation by pore plugging can be expected to be more severe for smaller pores, since the diffusion rate is slower and less $CaSO_4$ is required for blockage.

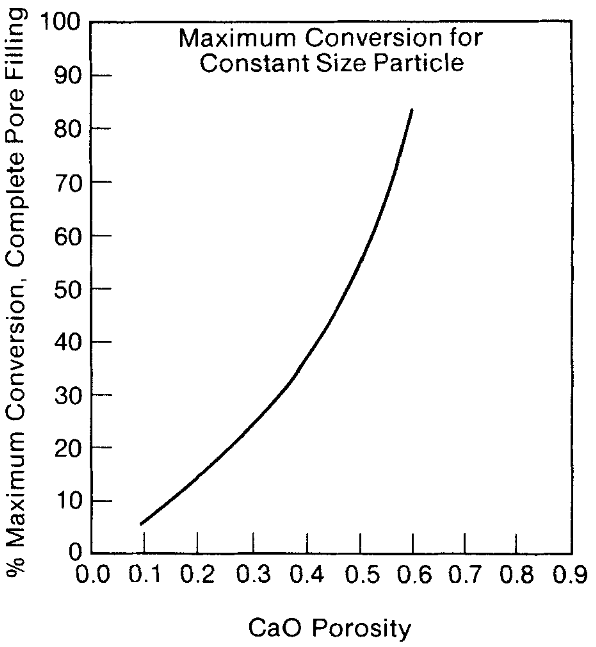

Figure 7. Theoretical maximum conversion of CaO to sulfate limited by available calcine pore space.

The degree of limitation of sulfation by pore mouth plugging varied widely among calcines produced from different sorbents (Table 4). The apparent activation energies (based on initial sulfation rates) ranged from negative values up to 92 kJ/mol. Activation energies below 40 kJ/mol are indicative of rapid premature pore mouth plugging, since they are significantly lower than expected for pore diffusion control. Saturated calcium utilizations also varied among calcines from different sorbents (17–80% at 1,075 K, Table 4), as did the dependence of the utilization on temperature. The wide variation in apparent activation energy and saturation utilization indicates varying severity of deactivation by pore mouth plugging among the different cal-

Table 4. Sulfation Performance of High Surface Area Calcines from 12 Test Sorbents

No.	Sorbent	Calcine Surface Area, m^2/g	$E_{apparent}$, kJ/mol*	Saturation Ca Conversion, % 1,075 K	1,175 K	1,275 K**
1	Dravo Maysville Limetsone, -100 mesh	55	64	39	36	33
2	Dravo Maysville Limestone, -325 mesh	35	63	50	50	36
3	Pfizer Marble White 200 Limestone	60	17	23	21	—
4	Warner Bell Mine Limestone	45	63	37	33	23
5	Mississippi R-1 Limestone	70	17	20	17	9
6	Genstar Apex Limestone	60	5.9	36	27	18
7	Utah Marblehead Limestone	65	62	31	20	11
8	Baker Reagent $CaCo_3$	55	92	45	36	—
9	Hommel #1974 Dolomite	70	Negative	32	22	—
10	Warner Dolomite	70	Negative	30	22	—
11	Dravo Longview Hydrated Lime	40	84	55	53	—
12	Pressure Hydrated Dolomite	45	88	80	80	—

*Apparent sulfation activation energy over 1,075–1,225 K.
**Runs at 1,275 K deviated from differential conditions.

cines. This occurred because of the variations in sorbent particle sizes and in calcine pore-size distributions with the different sorbents.

Pore-size distributions of selected calcines confirmed that calcines having more very fine pores are more adversely affected by pore mouth plugging. Figure 8 shows that a calcine from Genstar limestone (No. 6) had significantly finer pores (mostly 3–10 nm diameter) and less total pore volume than a calcine from Dravo limestone (No. 1). The calcined Dravo limestone had many pores in the 10–20 nm range. The Dravo calcine had a 55 m^2/g BET surface area, slightly lower than 60 m^2/g of the Genstar calcine. Both stones had similar average particle sizes (Table 1). Because of the larger pores in the Dravo calcine, it exhibited higher saturation calcium utilizations (Table 4), particularly at high temperatures (1,175 and 1,275 K), despite its lower surface area. The Genstar calcine showed a more severe reduction in saturation calcium utilization, from 36% to 18% with increasing temperature from 1,075 to 1,275 K. With the Dravo calcine, the reduction was only from 39% to 33% (Table 4). The apparent activation energy measured with calcined Genstar stone was 6.3 kJ/mol, far lower than the 64 kJ/mol observed with calcined Dravo stone (Table 4).

Comparison of Different Sorbents

Limestones and precipitated $CaCO_3$

Calcines from seven different limestones and one precipitated $CaCO_3$ sample tested exhibited widely varying saturation utilizations and initial reaction rates. Saturation utilizations at 1,075 K varied from 17% to 50% (Table 4). Apparent activation energies varied from 5.9 to 92 kJ/mol over 1,075–1,225 K (Table 4). These differences resulted from differences in the stone particle size (Table 1) and in the calcine intermediate pore structure. Calcine intermediate pore structure (surface area and pore size distribution) varied widely among different limestone precursors. However, the specific properties of the precurser $CaCO_3$ which lead to a favorable calcine pore structure were not clearly identified.

The precipitated $CaCO_3$ sample (No. 8) had a considerably higher $CaCO_3$ purity than the seven naturally occurring limestones tested. This reagent-grade sample showed relatively high initial activity and high saturation calcium utilizations (Table 4). On the other hand, Borgwardt et al. (1987) reported lower *intrinsic* activities for purer $CaCO_3$ samples, because the product-layer diffusivity, which determines the product-layer diffusion rate at the grains, was lower with less impurities. In the current tests conducted with pore diffusion resistance, product layer diffusion was not rate-limiting. Thus, calcine pore structure and particle size were more important factors affecting sorbent performance. The pure $CaCO_3$ had relatively small particles and produced a calcine pore structure favorable for pore diffusion.

Dolomitic stones

Calcines from two dolomitic stones tested were prone to deactivation by premature pore mouth plugging, presumably due to the presence of very small pores. Both showed negative apparent sulfation activation energies and low saturation calcium utilizations (22% at 1,175 K), as shown in Table 4. Both calcines had very high surface areas (70 m^2/g). Pore volume analysis of the calcine from the Hommel dolomite (No. 9) showed that it had over 85% of its pore volume in small pores, 2–10 nm in diameter (Figure 9).

Hydrated sorbents

Calcines derived from hydrated lime/dolomite showed better sulfation performance, in terms of both initial rate and saturation calcium utilization, than those derived for most limestones or dolomites. For the Dravo Longview hydrated lime (No. 11), saturated utilization was 55% at 1,075 K and dropped to 53% at 1,175 K (Table 4). The insensitivity of saturation conversion to temperature indicates the absence of significant calcine pore mouth plugging by the product. This is also indicated by the relatively high apparent activation energy (84 kJ/mol). The relatively low surface area for the calcine from the Longview hydrated lime (40 m^2/g) and the absence of deactivation by pore mouth plugging indicates that this calcine has larger pores than calcines for most of the limestones tested.

Figure 10 clearly shows the superior sulfation performance of a calcine from a pressure-hydrated dolomite (No. 12) to that from a dolomitic limestone (No. 9), the two calcines having roughly the same chemical composition. Saturation *calcium* uti-

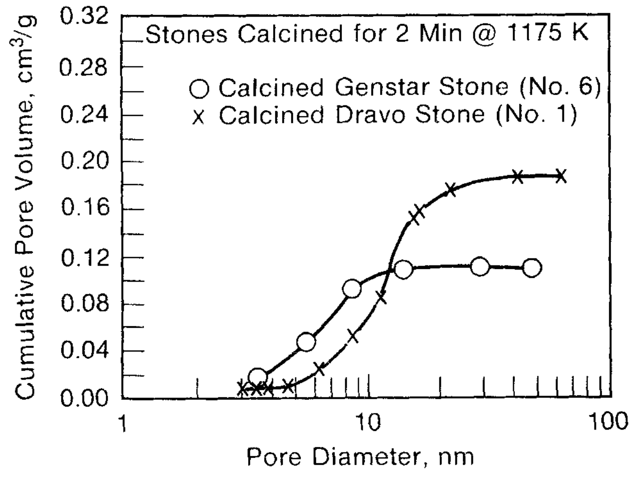

Figure 8. Cumulative pore volume distributions for calcines from two limestones.

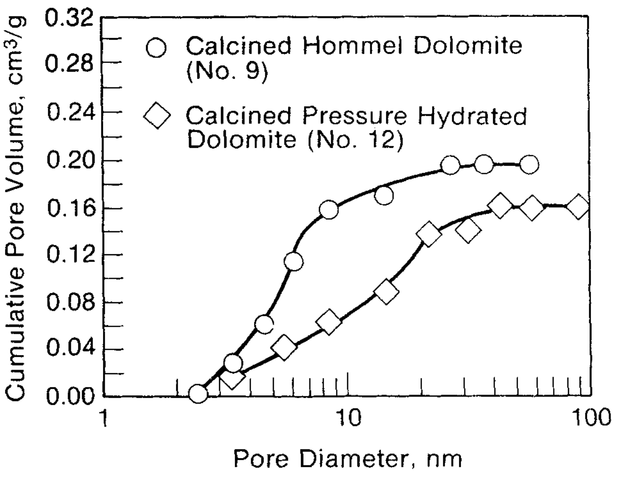

Figure 9. Cumulative pore volume distributions for calcines from two dolomitic sorbents.

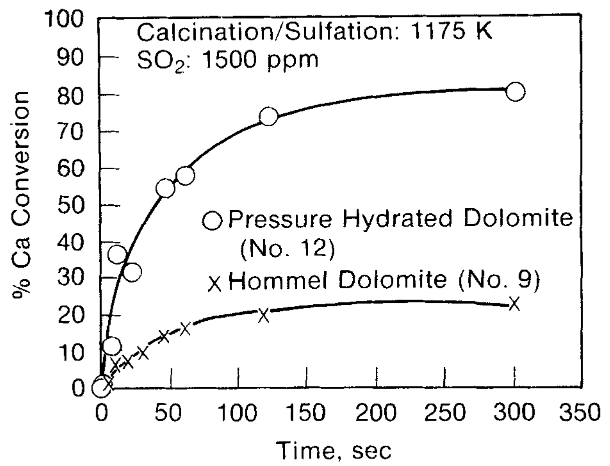

Figure 10. Comparison of sulfation activity of calcines from a dolomitic limestone and a pressure-hydrated dolomitic lime.

lizations at 1,175 K were 80% and 22% for the calcines from the pressure-hydrated dolomitic lime and the dolomitic stone, respectively. (The MgO in the calcines from the dolomitic sorbents did not capture significant SO_2 because of equilibrium limitations.) The saturated calcium utilization with the pressure-hydrated dolomite did not drop with temperature up to 1,175 K (Table 4). As shown in Figure 10, the initial sulfation rate for the calcine from the pressure hydrate was considerably higher than for that from the dolomitic limestone. The superior performance of the pressure-hydrated dolomite can be attributed in part to the formation of a favorable calcine pore structure. Pore volume analysis (Figure 9) showed that the calcine from the pressure hydrate had a broad pore-size distribution (4-40 nm diameter), with about 50% of its total pore volume contributed by pores 10 nm diameter and larger, as compared with the predominance of very small pores found in the calcine from the dolomitic stone.

Smaller CaO particle sizes also partly explain the superior performance of calcines from hydrated sorbents in the lab tests. Typical mean particle sizes for hydrated calcitic limes are 5 μm or less. All limestones tested had specific surface mean particle diameters larger than 8 μm.

The superior performance of calcines from hydrated sorbents observed in this lab study is consistent with observations in pilot and field tests of boiler injection.

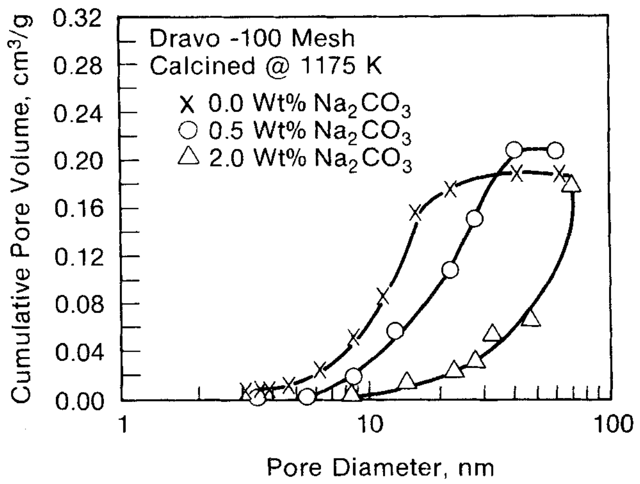

Figure 11. Effect of Na_2CO_3 additive on calcine pore volume distribution.

Effect of additive treating

Of several additives (Na_2CO_3, NaCl, $CaCl_2$, $FeCl_3$) evaluated, Na_2CO_3 was found to be the most effective in enhancing desulfurization performance of limestone. Both the initial reaction rate and saturation calcium utilization were increased substantially by Na_2CO_3. Additives were incorporated in limestone in small concentrations (0.25–5.0 g additive/100 g limestone) prior to calcination of the stone. The degree of enhancement increased with the Na_2CO_3 dosage up to 2 wt. % (i.e., 2 g/100 g limestone). The results indicate that the enhancement was due primarily to physical effects, that is, increasing the pore sizes in the calcine intermediate to a range more favorable for pore diffusion. The results further confirm the important role of calcine pore structure on sulfation activity under pore diffusion control. The observed calcine pore enlargement with Na_2CO_3 is consistent with reported alkali additive effects in fluidized-bed combustion studies (Gasner, 1979; Shearer, 1979; Shearer et al., 1979).

Additive effects were studied for two different limestones (Table 5), the Dravo (No. 1, Table 1) and the Genstar (No. 6). In most of the tests, the promoted limestone sample was prepared by the slurry mixing method described previously.

Figure 11 shows that sodium carbonate promotion of the Dravo stone significantly increased pore sizes of the calcine intermediate. With no additive, a calcine produced at 1,175 K had pores mostly in the 6-20 nm diameter range. With 0.5 wt. %

Table 5. Test Results with Na_2CO_3 Additive Promotion

		Calcine BET Surface Area (m^2/g) at Given Concentration of Na_2CO_3 in Limestone ($g\ Na_2CO_3/100\ g$ Stone)					% Saturation Ca Utilization at Given Concentration of Na_2CO_3 ($g\ Na_2CO_3/100\ g$ Stone)				
Limestone	Temp. K	0	0.25	0.5	2.0	5.0	0	0.25	0.5	2.0	5.0
Dravo Maysville -100	1,075	51	—	25	9	—	39	—	54	70	—
(Sorbent #1)	1,175	52	35	21	10	7	36	43	47	53	47
	1,275	36–45	—	21	6	—	33	—	32	44	—
Genstar Apex	1,075	60	—	23	—	—	36	—	48	—	—
(Sorbent #6)	1,175	58	—	29	10	—	27	34	40	61	—
	1,275	54	36	28	—	—	18	—	28	53	—

and 2 wt. % Na_2CO_3 incorporated in the stone by the slurry mixing method, the 1,175 K calcines had pores mostly in the 8–40 nm and 20–70 nm ranges, respectively. Because of the increased pore size, calcine surface areas decreased. The BET surface areas for these calcines were 52, 21 and 10 m^2/g, with Na_2CO_3 concentrations of 0, 0.5 and 2 wt. %, respectively (Table 5).

With the increase in calcine pore size with Na_2CO_3, the sulfation performance of the Dravo calcine was significantly enhanced (Figure 12). At 0.5 and 2 wt. % additive dosages, saturation calcium utilizations at 1,175 K increased from 36% (with no additive) to 47% and 53%, respectively. Initial sulfation rates also increased substantially. The Na_2CO_3 enhancement was observed over the entire test temperature range of 1,075 to 1,275 K (Table 5). Further increase above 2 wt. % did not provide additional enhancement. With 5 wt. % Na_2CO_3, the saturation calcium utilization (at 1,175 K with the Dravo calcine) was 47%, compared with 53% with 2 wt. % Na_2CO_3 (Table 5). The calcine with 5 wt. % Na_2CO_3 had a surface area of 7 m^2/g. This indicates that the surface area may have been reduced excessively, thus reducing the intrinsic rate at the grain surfaces. Even with 0.25 wt. % Na_2CO_3, some enhancement of sulfation was observed.

The substantial enhancement in sulfation performance by the Na_2CO_3 additive was due primarily to its effect on the calcine pore structure. The larger pores in the additive-promoted calcines were less hindered by pore diffusion resistance and less susceptible to premature pore mouth plugging by the $CaSO_4$ product. The small amounts of Na_2CO_3 used in the study could account only for an insignificant SO_2 capture as a sorbent (i.e., capture as Na_2SO_4 or Na_2SO_3).

The positive effect of Na_2CO_3 was also observed (Table 5) with the Genstar limestone (No. 6). At 1,175 K, the saturation calcium utilization increased from 27% with no additive to 61% with 2 wt. % Na_2CO_3. Initial reaction rate was also enhanced. Although pore volume distributions were not measured for the Genstar calcines, the observed drops in surface area (Table 5) indicate that the effect of Na_2CO_3 was again to increase calcine pore size and enhance pore diffusion.

In a few additional tests, the enhancement effect of Na_2CO_3 was observed by simply mixing dry Na_2CO_3 powder and limestone. However, the level of enhancement was not as great as when Na_2CO_3 was mixed with limestone in a slurry. For example, 0.5 wt. % Na_2CO_3 physically mixed with Dravo limestone (No. 1) at 1,175 K resulted in a decrease in calcine surface area to 32 m^2/g and an increase in saturated calcium utilization to 43%.

Other additives were not as effective as Na_2CO_3 in enhancing the sulfation performance of limestone. Sodium chloride (NaCl) showed some enhancing effect at some test conditions. For example, saturation conversion with a calcine from Dravo limestone (No. 1) increased from 36% to 42% at 1,175 K with 2 wt. % NaCl added to the stone prior to calcination (by mixing as a slurry). Calcium chloride ($CaCl_2$) and ferric chloride ($FeCl_3$) showed no consistent enhancement of sulfation performance.

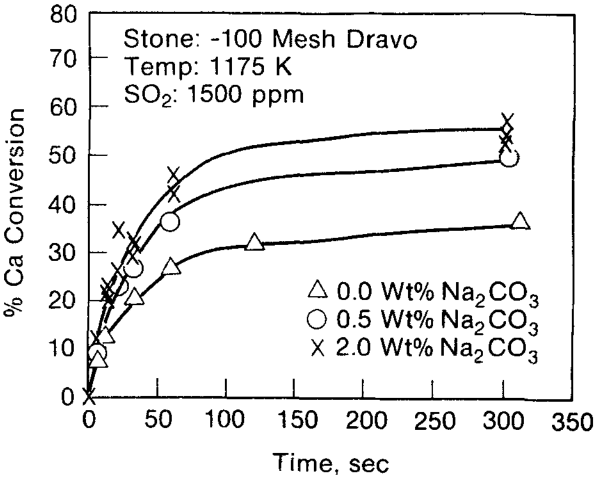

Figure 12. Enhancement of sulfation by Na_2CO_3 addition to limestone.

Conclusions

The results of this lab study indicate that the SO_2 removal rate for a boiler injection sorbent, such as pulverized limestone, dolomite, or hydrated lime, is limited by SO_2 pore diffusion in the intermediate calcine generated in the boiler. Additionally, pore mouth plugging by the product $CaSO_4$ further limits the reaction rate and lowers the saturation calcium utilization level. Because of the strong pore diffusion control and pore mouth plugging effect, particle size of the sorbent and pore size distribution of the intermediate calcine are the most important properties determining the sorbent performance for boiler SO_2 capture. At 1,175 K, the initial reaction was inversely proportional to the particle size for the limestones having 8–112 μm average particle diameters. A calcine having pores predominantly less than 10 nm size showed significantly reduced saturation calcium utilization due to pore mouth plugging as the temperature was increased to 1,275 K, the highest temperature used in this study.

The pore-size distribution of the intermediate calcine depended on limestone source and, thus, prescreening of candidate limestones from different sources is important for the boiler injection application. Hydrated limes were superior to limestones or dolomites, since hydrates consist of smaller particles and they produce calcines with larger pores. Na_2CO_3 treatment substantially improved the desulfurization performance of limestone in terms of initial reaction rate and saturation utilization. Up to 2 wt. % treatment of Na_2CO_3 increased the pore sizes from mostly 6–20 nm to 20–70 nm. The increase in the pore size was accompanied by a reduction in the calcine BET surface area from 52 to 10 m^2/g. These results indicate that the surface area, the calcine property determining the intrinsic reaction rate, is not an important factor for calcine performance under pore diffusion control.

In the lab tests, reaction rates limited by the intrinsic rate were measured only with low surface area (less than 15 m^2/g) calcines and below 1,075 K, a temperature below the range of boiler sorbent injection.

Notation

C = concentration of diffusing species at outer surface of product layer, mol/m^3
D_i = average particle diameter in a particular size cut (i), μm
D_p = particle diameter, μm
D_s = product-layer diffusivity, m^2/s
D_o = preexponential factor for diffusivity, m^2/s
E = activation energy, kJ/mol
E_a = apparent activation energy, kJ/mol
E_d = activation energy for diffusion, kJ/mol

k_d = rate constant in unreacted core model, Eqs. 1, 2 and 3, s^{-1}
M = molecular weight CaO, g/mol
n = reaction order in SO_2 partial pressure
P_{SO_2} = partial pressure of SO_2 in gas stream, Pa
R = gas constant, 8.319×10^{-3} kJ/mol·K
S = surface area per unit mass of calcine, m^2/g
t = contact time, s
T = absolute temperature, K
X = fractional calcium conversion, mol S captured per mol Ca
Y_i = weight fraction of particles in a particular size cut (i)

Greek letters

ρ = absolute density of calcine, g/m^3

Literature Cited

Bardaki, T., "Diffusional Study of the Reaction of Sulfur Dioxide with Reactive Porous Matrices," *Thermochimica Acta,* **76,** 287 (1984).

Barrett, E. P., L. G. Joyner, and P. P. Halenda, "Determination of Pore Volume and Area Distributions in Porous Substances: I. Computations from Nitrogen Isotherms," *J. Am. Chem. Soc.,* **73,** 3155 (1951).

Beittel, R., J. P. Gooch, E. B. Dismukes, and L. J. Muzio, "Studies of Sorbent Calcination and SO_2 Sorbent Reactions in a Pilot-Scale Furnace," *Proc. Joint Symp. on Dry SO_2 and Simul. SO_2/NOx Control Technol.,* San Diego, CA, 16-1 (1984).

Bhatia, S. K., and D. D. Perlmutter, "A Random Pore Model for Fluid-Solid Reactions: II. Diffusion and Transport Effects," *AIChE J.,* **27,** 247 (1981).

Borgwardt, R. H., "Calcination Kinetics and Surface Area of Dispersed Limestone Particles," *AIChE J.,* **31,** 103 (1985).

———, "Kinetics of the Reaction of SO_2 with Calcined Limestone," *Environ. Sci. Technol.,* **4,** 59 (1970).

Borgwardt, R. H., and R. D. Harvey, "Properties of Carbonate Rocks Related to SO_2 Reactivity," *Environ. Sci. Technol.,* **6,** 350 (1972).

Borgwardt, R. H., K. R. Bruce, and J. Blake, "An Investigation of Product-Layer Diffusivity for CaO Sulfation," *Ind. Eng. Chem. Res.,* **26**(10), 1993 (1987).

Borgwardt, R. H., N. F. Roach, and K. R. Bruce, "Method for Variation of Grain Size in Studies of Gas-Solid Reactions Involving CaO," *Ind. Eng. Chem. Fund.,* **25**(1), 165 (1986).

Borgwardt, R. H., and K. R. Bruce, "Effect of Specific Surface Area on Reactivity of CaO with SO_2," *AIChE J.,* **32,** 239 (1986).

Bortz, S., and P. Flament, "Recent IFRF Fundamental and Pilot Studies on the Direct Sorbent Injection Process," *Joint Symp. on Dry SO_2 and Simul. SOx/NOx Control Technol.,* San Diego, CA (1984).

Chang, E. Y., and G. Thodos, "Complex Nature of the Sulfation Reaction of Limestones and Dolomites," *AIChE J.,* **30**(3), 450 (1984).

Ciambelli, P., et al., "Sulfur Dioxide Reactivity of Carbonate Rocks," *Fuel,* **64,** 816 (1985).

Cole, J. A., J. C. Kramlich, W. R. Seeker, G. D. Silcox, G. H. Newton, D. J. Harrison, and D. W. Pershing, "Fundamental Studies of Sorbent Reactivity in Isothermal Reactors," *Joint Symp. on Dry SO_2 and Simul. SO_2/NOx Control Technol.,* Raleigh, NC (1986).

Dogu, T., "The Importance of Pore Structure and Diffusion in the Kinetics of Gas-Solid Non-Catalytic Reactions: Reaction of Calcined Limestone with SO_2," *Chem. Eng. J.,* **21,** 213 (1981).

Fink, C. E., N. S. Harding, B. J. Koch, D. C. McCoy, R. M. Statnick, and T. J. Hassell, "Demonstration of Boiler Limestone Injection in an Industrial Boiler," *Joint Symp. on Dry SO_2 and Simul. SO_2/NOx Control Technol.,* San Diego, CA (1984).

Gasner, L. L., "The Addition of Salt to Fluidized Bed Combustors," *Proc. Int. Symp. on Salt,* No. Ohio Geological Soc., 439 (1979).

Hartman, M., and R. W. Coghlin, "Reaction of Sulfur Dioxide with Limestone and the Influence of Pore Structure," *Ind. Eng. Chem. Process Dev.* **13,** 148 (1974).

———, "Reaction of Sulfur Dioxide with Limestone and the Grain Model," *AIChE J.,* **22**(3), 490 (1976).

James, N. J., and R. Hughes, "Rates of SO_2 Adsorption in Calcined Limestones and Dolomites," Univ. of Salford, *Int. Conf. on Control of Gaseous Sulfur and Nitrogen Compound Emissions,* Salford, England (1976).

Kirchgessner, D. A., and B. K. Gullett, "Physical Parameters Governing Reactivity of $Ca(OH)_2$ with SO_2," *Joint Symp. on Dry SO_2 and Simul. SO_2/NOx Control Technol.,* Raleigh, NC (1986).

Levenspiel, O., *Chemical Reaction Engineering,* Wiley, New York, **469** (1972).

Pigford, R. L., and G. Sliger, "Rate of Diffusion Controlled Reaction Between a Gas and a Porous Solid Sphere." *Ind. Eng. Chem. Process Dev.,* **12,** 85 (1973).

Potter, A. E., "Sulfur Oxide Capacity of Limestones," *Am. Ceramic Soc. Bull.,* **48,** 855 (1969).

Shearer, J. A., et al., "The Effect of Sodium Carbonate Additive on the Reaction of SO_2/O_2 Mixtures with Carbonate Rocks," Argonne National Laboratory, Report ANL/CEN/FE-79-11 (1979).

Shearer, J. A., "The Effect of $CaCl_2$ Additive on the Reaction of SO_2/O_2 Mixtures with Carbonate Rocks," Argonne National Laboratory, Report ANL/CEN/FE-79-7 (1979).

Snow, G. C., J. M. Lorrain, and S. L. Rakes, "Pilot Scale Furnace Evaluation of Hydrated Sorbents for SO_2 Capture," *Joint Symp. on Dry SO_2 and Simul. SO_2/NOx Control Technol.,* Raleigh, NC (1986).

Stouffer, M. R., and H. Yoon, "Laboratory Calcination and Sulfation Studies for Boiler Limestone Injection," Workshop on Coal Liquid and Alternate Fuels Technology, Halifax, Nova Scotia, Canada (Sept., 1986).

Szekely, J., and J. W. Evans, "A Structural Model for Gas-Solid Reactions with a Moving Boundary," *Chem. Eng. Sci.,* **25,** 1091 (1970).

Szekely, J., J. W. Evans, and H. Y. Sohn, *Gas-Solid Reactions,* Academic Press, New York (1976).

Manuscript received Oct. 24, 1988, and revision received Apr. 20, 1989.